Randomly Disordered Glass-Air Optical Fiber Imaging Based on Deep Learning

Jian Zhao,[1,*] Yangyang Sun,[1] Zheyuan Zhu,[1] Jose Enrique Antonio-Lopez,[1] Rodrigo Amezcua Correa,[1] Shuo Pang[1] and Axel Schülzgen[1]

[1]CREOL, College of Optics and Photonics, University of Central Florida, Orlando, FL 32816, USA

**Corresponding author: JianZHAO@knights.ucf.edu*

Abstract: We demonstrate that images can be reconstructed for objects away from the imaging plane without any distal optics by combining deep neural networks with meter-long glass-air disordered optical fibers. This imaging system is bending-independent.

OCIS codes: (060.2310) Fiber Optics; (060.2350) Fiber optics imaging; (060.4005) Microstructured fibers;

1. Introduction

Image transport using disordered optical fibers based on transverse Anderson localization (TAL) has been investigated in detail recently [1-5]. It has been proven that image quality obtained after transport through glass-air Anderson localized optical fibers (GALOFs) can be comparable to or better than that after transport through some of the best commercial multicore imaging fibers [1]. Moreover, the image transport through GALOFs is bending-independent due to single mode properties of the transversally localized states in the fiber [1,3,5]. The GALOF shows great potential in optical-fiber-based endoscope applications. However, the structural parameters of current GALOFs are still less than perfect, which limits the quality of transported images. In addition, the imaging plane is located directly at the GALOF's input facet unless distal optics are added. For objects away from the fiber input facet only a blurred image is observed at the proximal facet. Recent progress of deep-learning based computational imaging can be utilized to overcome these difficulties [6,7]. In this work, we demonstrate experimentally that high-quality bending-independent image transport can be obtained through a meter-long GALOF even if the objects are located 4 mm away from the imaging plane without any distal optics. This has been achieved by training deep neural networks (DNNs) to reconstruct the images.

2. DNN training, experiment and results

A DNN attempts to generate a computational architecture that maps all input in a test set to their corresponding outputs based on a given training set. In our experiment, images of objects located at different working distances are transported through 90 cm of straight or bent GALOF and subsequently recorded by a CCD camera. The object reconstruction process can be described as:

$$X = HY_{measure} \quad , \tag{1}$$

where $Y_{measure}$ is the measured image matrix and X is the reconstructed image matrix. The pair (X, $Y_{measure}$) corresponds to a test set, and H is an inverse operator that gives an estimation of the original object from the measurement. In past years, obtaining the inverse operator by solving the optimization problem has been studied in detail [8,9]. However, it requires accurate modeling and prior knowledge of the object. In contrast, DNNs can learn H from a provided training set and no prior knowledge of the object is required. The method applied here is an extension of a recent DNN study [7] which uses a convolutional residual neural network. The architecture of our DNN is shown in Fig.1. The input layer is a 448×448×1 pixel image cropped from the measured image. Then it is successively connected by five residual blocks of convolution+down-sampling (Fig. 1 blue arrows) followed by two residual blocks of deconvolution+up-sampling (Fig. 1 red arrows) and a single final standard residual block (Fig. 1 black arrow). At the very last layer of our DNN, the output represents an estimation of the object. The connection weights are trained by backpropagation on the mean absolute error (MAE) between the network output images and the nominal appearance of the training images (Fig. 1 double-sided arrow) described as: $|X_{train} - G|/(wh)$, where w and h are the width and height of the output image, respectively, X_{train} is the output matrix of the last layer and G is the ground truth value matrix.

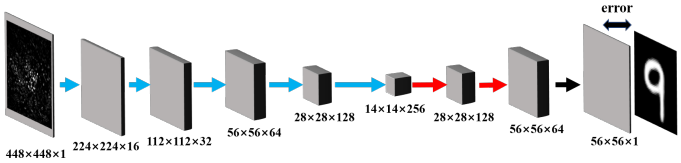

Fig. 1. Schematic of our DNN architecture.

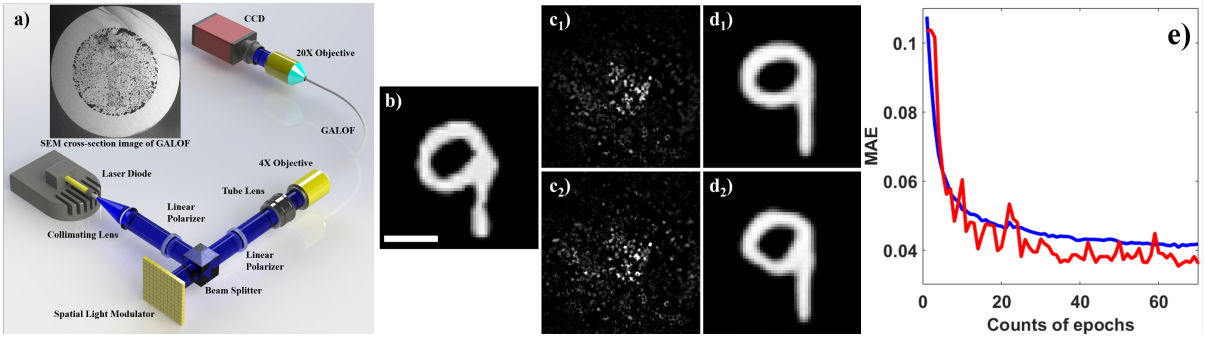

Fig. 2. a) Imaging setup and SEM cross-section image of GALOF. The outer diameter of the GALOF is 414 μm and the diameter of the disordered core is 278 μm. The air-hole-fraction in the core is 28.5%. The air-hole feature sizes range from 0.8 μm to over 10 μm with a maximum in the size distribution around 1.6 μm. b) A sample object from the MNIST database of handwritten digits. Image b) is projected on the plane being 4 mm away from the GALOF input facet. c_1) Image of b) after transport through straight 90 cm of GALOF, and d_1) is the corresponding reconstructed image after DNN training. c_2) Image of b) after transport through the same GALOF which has been bent to form a 90 degree turn with a bend radius of 32 cm and d_2) is the corresponding reconstructed image using the same DNN training applied to the straight GALOF. The scale bar in b) is 45 μm. e) Mean absolute error (MAE) curve. Blue curve obtained from the training set. Red curve obtained from the validation sets. There are 70 epochs in total.

The GALOF was fabricated at CREOL using fused-silica tubes and the stack-and-draw method. The experimental arrangement and a SEM image of the GALOF cross-section are shown in Fig. 2(a). 405 nm laser light delivered by a single mode fiber is collimated by a lens (50 mm focal length). Then the light goes through the first polarizer oriented 45° with respect to the extraordinary axis of the spatial light modulator (SLM). The SLM (1920x1152 XY Spatial Light Modulator, Meadowlark Optics) is modulated by 8-bit grayscale input images (MNIST Digits). After reflection from the SLM, the beam goes through a second polarizer with the same polarization orientation as the first one. Then the imaging area of the SLM is projected onto the GALOF input facet directly by the combination of a tube lens and a 4x objective. At the output end of the GALOF the fiber facet is projected onto a CCD by a 20x objective. 4000 images from the MNIST dataset are fed into the system when the GALOF is straight to generate corresponding raw intensity images. These 4000 image pairs are used to train our DNN. A second set of 200 different raw intensity images are collected as the validation set for the straight GALOF. A third set of another 200 different raw intensity images are collected as the test set for both straight GALOF and bent GALOF. We adopted an Adam optimizer in tensor flow with a batch size of 40 for the training set. The learning rate is set to 0.001. The training time is 63 minutes on two GPUs (GeForce 1080 Ti). The neural network was trained for 70 epochs with shuffling at each epoch. Image reconstruction results are shown in Fig 2. Fig. 2 b), c) and d) show the original object, raw intensity images and the corresponding reconstructed images, respectively. The reconstruction time is 4.23 ms for each test image. Comparing raw intensity images and the corresponding reconstructed images, it is apparent that our trained DNNs are able to recover the true images remarkably well and the reconstruction process is independent of GALOF bending. Importantly, no retraining is required to reconstruct images transported through the bent GALOF. The MAE curves for both training set and validation set are shown in Fig. 2(e). The error value is obtained by averaging MAE in the last batch of each epoch. Based on the MAE curves, we can conclude that convergence is achieved and there is no overfitting. The average values of the MAE for our test sets are 0.0354 and 0.0508 for straight and bent GALOF, respectively.

3. Conclusion

In conclusion, we demonstrate a bending-independent disordered optical fiber based imaging system where a trained DNN is utilized to reconstruct objects being away from input imaging plane without any distal optics.

4. References

[1] J. Zhao, J. E. Antonio-Lopez, Z. Zhu, D. Zheng, S. Pang, R. A. Correa, and A. Schülzgen, "Image Transport Through Meter-Long Randomly Disordered Silica-Air Optical Fiber," Sci. Rep. **8**, 3065, doi:10.1038/s41598-018-21480-0 (2018).
[2] S. Karbasi, R. J. Frazier, K. W. Koch, T. Hawkins, J. Ballato, and A. Mafi, "Image transport through a disordered optical fibre mediated by transverse Anderson localization," Nat. Commun. **5**, 3362 doi:10.1038/ncomms4362 (2014).
[3] G. Ruocco, B. Abaie, W. Schirmacher, A. Mafi, and M. Leonetti, "Disorder-induced single-mode transmission," Nat. Commun. **8**, 14571 doi:10.1038/ncomms14571 (2017).
[4] J. Zhao, J. E. Antonio-Lopez, R. A. Correa, A. Mafi, M. Windeck, and A. Schülzgen, "Image Transport Through Silica-Air Random Core Optical Fiber," in "CLEO: Science and Innovations," (Optical Society of America, 2017), paper JTu5A.91.
[5] J. Zhao, J. E. Antonio-Lopez, R. A. Correa, D. Zheng, and A. Schülzgen, "Image Transport Through Meter-Long Silica-Air Disordered Optical Fiber," 5th Workshop on Specialty Optical Fibers, paper: 10 (2017), to be published in Proceedings SPIE.
[6] A. Sinha, J. Lee, S. Li, and G. Barbastathis, "Lensless computational imaging through deep learning," Optica **4**,1117-1125 (2017).
[7] R. Horisaki, R. Takagi, and J. Tanida, "Learning-based imaging through scattering media," Opt. Express **24**, 13738-13743 (2016).
[8] Y. Sun, X. Yuan, and S. Pang, "High-speed compressive range imaging based on active illumination," Opt. Express **24**, 22836-22846 (2016)
[9] Y. Sun, X. Yuan, and S. Pang, "Compressive high-speed stereo imaging," Opt. Express **25**, 18182-18190 (2017).